Transition of Gas-Liquid Stratified Flow in Oil Transport Pipes

D. Lakehal*[a], M. Labois[a], D. Caviezel[a], and B. Belhouachi[b]

[a]*ASCOMP GmbH, Technoparkstr. 1, Zurich, CH 8005, Switzerland*
[b]*Imperial College London, Prince Consort Road, London SW7 2BY, UK*

انتقال التدفق الطبقي للغاز والسائل في أنابيب نقل النفط

د. الأكح*أ ، م. لوبوازم أ، د. كافيزل أ و ب. بلهوتشي ب

الخلاصة: نناقش في هذه الورقة نتائج المحاكاة الواسعة النطاق لظاهرة انتقال الجريان الطبقي للغاز والسائل في أنابيب نقل النفط تحت ظروف تدفق مضطربة. وقد تمت معالجة السطح الفاصل بين الغاز والسائل بطريقة حديثة تسمى طريقة خطوط المستويات. وقد أوضحت الدراسة أن هذه الطريقة قادرة على تمثيل الجريان الطبقي بدقة أكبر من تلك النماذج المستخدمة في ثنائي الموائع متوسط الأطوار. وقد بينت الدراسة أن انتقال الجريان من الطبقي إلى السبيكي (slug) يحدث نتيجة لاندماج أمواج الجريان ذات النسق الثانوي (الموجات القصيرة) مع تلك ذات النسق الأول (الموجات طويلة السعة). وقد تبين أن النموذج الرياضي المستعمل في هذه الدراسة يستطيع التنبؤ بخواص الجريان عامة كظهور الجريان السبيكي وسرعته. وفي حاله أخرى تمت دراستها في جامعة الامبريال في لندن تبين أن هذا النموذج يستطيع التنبؤ بظهور أنواع أخرى من الجريان السبيكي في الجريان الطبقي للماء و الغاز كذاك المسمى بالجريان السبيكي التشغيلي الذي يتشكل في بداية الأنبوب بسبائك من الماء بطول قطري ٢ –٤ وكان أقل قطر هو ١ – ١٫٥ والمسماه بالسبائك التشويشية و المتميزة بنسبة ماء تصل من ٨٠ إلى ٩٠٪. وقد تبين أن النموذج الرياضي يستطيع التنبؤ بتكرار ظهور الجريان السبيكي بدقه عالية. وقد أظهرت نتائج المحاكاة الرياضية أن العوامل ذات التاثير الكبير على الظاهرة المدروسة في هذه الورقة هي نوعية التدفق وطول الأنبوب ونسبة الماء.

المفردات المفتاحية: الجريان الطبقي، الجريان ثنائي الاطوار، طريقة خطوط المستويات

Abstract: Large-Scale Simulation results of the transition of a gas-liquid stratified flow to slug flow regime in circular 3D oil transport pipes under turbulent flow conditions expressed. Free surface flow in the pipe is treated using the Level Set method. Turbulence is approached via the LES and VLES methodologies extended to interfacial two-phase flows. It is shown that only with the Level Set method the flow transition can be accurately predicted, better than with the two-fluid phase-average model. The transition from stratified to slug flow is found to be subsequent to the merging of the secondary wave modes created by the action of gas shear (short waves) with the first wave mode (high amplitude long wave). The model is capable of predicting global flow features like the onset of slugging and slug speed. In the second test case, the model predicts different kinds of slugs, the so-called operating slugs formed upstream that fill entirely the pipe with water slugs of length scales of the order of 2-4 D, and lower size (1-1.5 D) disturbance slugs, featuring lower hold-up (0.8-0.9). The model predicts well the frequency of slugs. The simulations revealed important parameter effects on the results, such as two-dimensionality, pipe length, and water holdup.

Keywords: Stratified flow, Two-phase flow, Level-set method

1. Introduction

Liquid-liquid flows appear in various industrial processes and in the petroleum industry in particular, where mixture of gas with associated liquids (oil, condensate and/or water) are produced and transported together. During their co-current flow in a pipe the deformable interfaces requires various characteristdistributions called flow regimes or flow patterns (Hewitt 1982). Understanding the transition from stratified flow to slug flow is important in hydrocarbon transportation systems, and has constantly stimulated the research in this direction (Valluri *et al*. 2008). Slug flow is a commonly observed pattern in horizontal and

---

*Corresponding author's e-mail: lakehal@ascomp.ch

near horizontal gas liquid flows. It is the regime with large coherent disturbances, causing large pressure fluctuations and variations in the flow rates that can affect process equipment. It is also characterized by intermittent appearance of aerated liquid masses that entirely fill the pipe cross-section and travel downstream at a large velocity. Earlier techniques for the prediction of slugs were based on various linear stability theories. The transition from stratified to slug flow regime has often been associated with the sudden growth of interfacial waves due to the Kelvin-Helmholtz instability. The onset of this instability for long waves has early been determined analytically assuming a continuous growth of a small-amplitude long wave into a slug, driven by Kelvin-Helmholtz instabilities (Taitel and Dukler 1976). Wall shear and interfacial stress were later accounted for, but the long-wave assumption was retained, facilitating an integral momentum balance. Although the criteria for linear instability obtained in these early theoretical studies show good agreement with experimental conditions at the onset of slug formation, the underlying assumptions have been increasingly undermined by subsequent work and now seem unlikely to be justifiable. Other authors (Valluri *et al*. 2008) report observations invalidating the assumption that a single long wave develops continuously into a slug (Lin and Hanratty 1986).

This slug formation subject is addressed here by means of large scale simulation using the CMFD code (TransAT of ASCOMP GmbH, 2010), combining the Level Set method for interface tracking and LES/VLES for turbulence. This model combination of ITM and LES/VLES is referred to as LEIS, short for Large Eddy and Interface Simulation (Lakehal 2010). We discuss the 3D results of flow transition to slug in two different pipe configurations under turbulent flow conditions. Turbulence is approached via the LES and V-LES methodologies extended recently (Liovic and Lakehal 2007) to interfacial two-phase flows. The simulations were conducted 3D.

2. The Mathematical Model

In TransAT, the incompressible two-fluid flows are represented by a single equation by a technique known as the Interface Tracking Method (ITM). For more details, the reader can refer to (Lakehal *et al*. 2002). The equations are of the form:

$$\frac{\partial \rho}{\partial t} + \mathbf{u}\,\nabla \rho = 0$$

$$\frac{\partial(\rho\,\mathbf{u})}{\partial t} + \nabla.\left(\rho\,\mathbf{u}\,\mathbf{u}\right) = -\nabla p + \nabla.\,\mu\left(\nabla\mathbf{u} + \nabla^T\mathbf{u}\right) + F_b + F_w + F_s$$

(1)

where u stands for the fluid velocity and p for the pressure, ρ is the density, and μ is the viscosity. The source terms in the RHS of the momentum equation represents the body force, F_b, the wall shear, F_w, and the surface tension, F_s. Material properties are updated locally based on a phase marker field, denoted here by the level-set function ϕ (Sussman *et al*. 1994). ϕ is a distance function, whose value represents the distance to the interface. The interface itself has a value of zero, is positive on one side and negative on the other. Other material properties like viscosity, thermal conductivity and heat capacity are also updated in the same way. TransAT uses the Immersed Surfaces Technology (IST), whereby the wall shear (F_w) appears explicitly in the equations based on the solid level-set function ϕ_s that defines solid obstacles (in addition to the gas-liquid function ϕ). To track the interface and update material properties, a topology equation is solved for the level-set function ϕ:

$$\frac{\partial \phi}{\partial t} + \mathbf{u}\,.\nabla \phi = 0$$

(2)

Conceptually, ITMs are capable of capturing the topology of interfaces and resolving accurately the interfacial boundary layers, independently from the Reynolds number. But since full DNS resolving all turbulence and interface motions is practically elusive, one is forced to solve the flow using statistical models like RANS, or LES, solving directly for super-grid scale and modelling unresolved or sub-grid scales (SGS). For turbulent interfacial flows, use should be made of the filtered form of the equations above (Lakehal 2010; Liovic and Lakehal 2007). This is now known as the LEIS, short for Large Eddy & Interface Simulation, in which turbulent scales and interface deformations larger than the grid size are directly solved, whereas sub-scales are modelled (Lakehal 2010; Liovic and Lakehal 2007). Because statistically steady-state flow conditions are difficult to attain in 3D, recourse is made here of the V-LES (instead of LES), where the flow-dependent cut-off filter is larger and independent from the grid. Although contradictory in terms of scale separation, one actually could resort to RANS closure models to deal with turbulence as well, at the expense of affecting the degree of interface topology resolution; higher eddy viscosity levels at the interface could hamper the high-frequency surface motions, *i.e.* wrinkling. Be it as it may, advancing the RANS form of the above system of equation in time is referred to as URANS.

3. The Numerical Approach

The CMFD code (TransAT 2010) developed at

ASCOMP is a multi-physics, finite-volume code based on solving multi-fluid Navier-Stokes equations. The code uses structured meshes, though allowing for multiple blocks to be set together. MPI and OpenMP parallel based algorithms are used in connection with multi-blocking. The grid arrangement is collocated and can thus handle more easily curvilinear skewed grids. The solver is pressure based (Projection Type), corrected using the Karki-Patankar technique for subsonic to supersonic compressible flows. High-order time marching and convection schemes can be employed; up to third order Monotone schemes in space. Multiphase flows can be tackled using (i) interface tracking techniques for both laminar and turbulent flows (Level Set, VOF with interface reconstruction, and Phase Field), (ii) N-phase, phase-averaged mixture model with Algebraic Slip, and (iii) Lagrangian particle tracking (one-to-four way coupling). As to the level set, use is made of the 3rd order Quick scheme for convection, and 3rd order WENO for re-distancing. Mass conservation is enforced using global and local mass-conserving schemes (Lakehal *et al* 2002). To mesh complex geometries, use is made of the Immersed Surfaces Technology (IST) developed by implemented in the code (Labois and Lakehal 2011).

4. Slug Formation In Condensation-Induced Waterhammer

4.1 Problem Description

The experiment of Martin *et al.* (2005) was designed for the purpose of investigating the phenomenon of condensation-induced waterhammer in an ammonia refrigeration system. Waterhammer was initiated by introducing warm ammonia gas over static subcooled ammonia liquid placed in a horizontal carbon steel pipe 6.0 m in length. The only data used for comparison with the simulation include the isothermal subsonic case, with no condensation. The apparatus was designed to simulate an industrial environment whereby ammonia liquid is standing in a partially-filled horizontal pipe in thermal equilibrium with ammonia gas above it. The essential elements of the test setup consist of a horizontal pipe and a high pressure tank containing warm ammonia gas, as shown in Fig. 1. The test pipe has a nominal diameter of 150 mm and length of 6 m, made of 80 carbon steel, having internal diameter of 146.3 mm, and wall thickness 11.0 mm. The pressure tank contains warm ammonia gas on top of liquid in thermal equilibrium at ambient conditions inasmuch as the entire test facility was outdoors. Between the pressure tank and the test pipe were three valves and a metering orifice. The angle valve remained fully open, while flow was initiated by a solenoid valve for a given position of the throttle valve. The ammonia in the insulated test pipe was

introduced from an ancillary system containing a compressor, an auxiliary tank, and another tank for purging non-condensable gases. For each test, care was exercised to transfer ammonia liquid to or from the test pipe to establish the desired depth and equilibrium temperature.

Instrumentation consisted of an orifice meter to determine the transient mass flow rate utilizing both upstream P0 and differential pressure transducers *PΔ*. In order to calculate the mass flow rate through the orifice, which was calibrated with water, the upstream temperature was monitored by RTD1. Another pressure transducer (PD) was located in the downcomer. The initial liquid temperature within the test pipe was recorded by RTD2, mounted on the bottom of the pipe. For the measurement of waterhammer or shock pressures four piezoelectric pressure transducers - PCB1, PCB2, PCB3, and PCB4 - were mounted as shown. The first three piezoelectric transducers were on the bottom of the pipe, while PCB4 was mounted on the pipe centerline at the end cap. In order to determine the gas pressure within the test section during the transient event four diaphragm differential pressure transducers - labeled PACE1, PACE2, PACE3, and PACE4 were mounted on the top of the pipe, as shown in Fig. 1. By maintaining one side of the diaphragm open to the atmosphere and the other side connected to the top of the pipe gage pressures were measured during the test. The test procedure consisted of reducing the liquid and gas temperature within the test pipe to the desired value by means of a compressor.

4.2 Simulation Setup

A full 3D computational domain is considered in these simulations. A portion of the grid is shown in Fig. 2. The pipe length is 6.3m, and the diameter is 0.14 m. The multi-block grid strategy is used to cover the domain with adjacent sub-domains (coloured differently). Here boundary fitted grids were used rather than the IST. The blocks are distributed between 12 processors for MPI parallel execution. The results presented here were obtained for a grid composed by 360,000 curvilinear cells distributed over 12 blocks. The LEIS approach was employed here, relying on the Level-Set technique for interface tracking. Sub-grid scale (SGS) modelling was achieved using the MILES approach (Lakehal 2010), where the diffusive effects of unresolved turbulence motion is left to the scheme. The inflow boundary conditions involve fixing the superficial gas and liquid velocities and the void fraction as specified in the experiments. The right-end of the cap was left open now since we deal with the non-phase case; pressure boundary conditions were used, in combination with a special scheme for the void fraction to control global and phase-specific volume conservation. Specifically at the inflow, we have set the
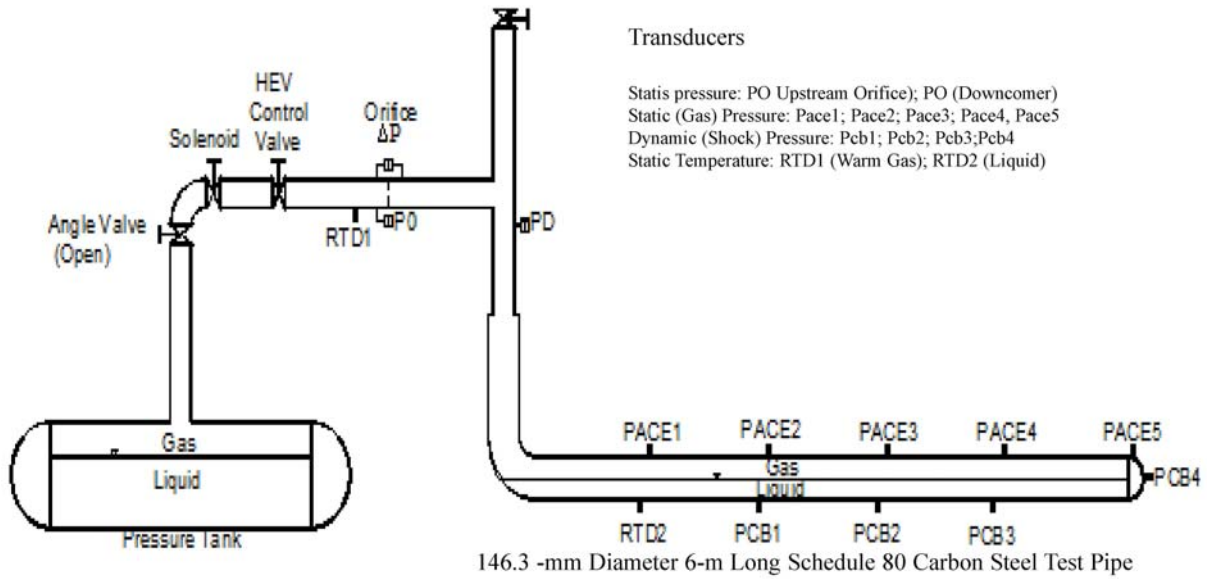
D. Lakehal, M. Labois, D. Caviezel and B. Belhouachi

Figure 1. Schematic of test pipe, orifice, and pressure tank

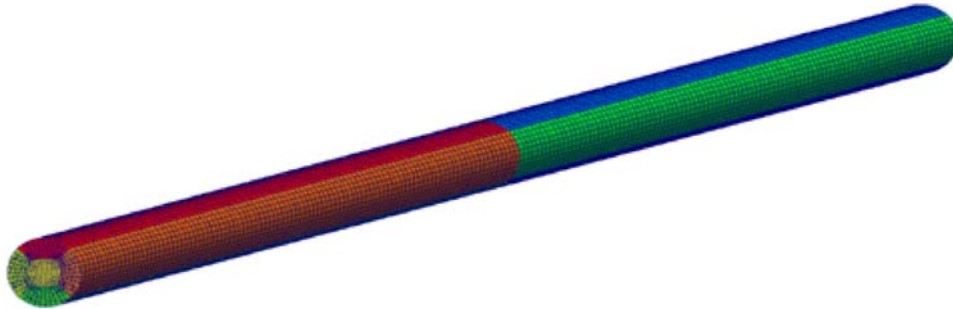**Figure 2.** Computational multi-block grid using BFC

following values for the turbulent flow conditions: gas superficial velocity U_{sG} = 14m/s; liquid superficial velocity U_{sL} = 0.5m/s; void fraction = 50%. An initial flow disturbance was applied in the flow domain, based on the wall shear Reynolds number.

4.3 Simulation Results

The development of waves in the gas liquid pipe flow is shown for the case of 14m/s inlet gas velocity and 50% void fraction in the next figures. Figure 3 shows successive surface displacements predicted at various successive time steps. A first wave mode is seen to develop under the action of pressure and inter-facial shear at about 1.5D from the inflow plane.

The surface of this wave is clearly three-dimensional. Small slope waves are developed further downstream. A second mode is formed in the wake of the first one, which seems to merge further downstream just before slug formation. The slug forms only far downstream at six pipe-diameters from the inflow. The difference with earlier 2D simulations (results not

shown here) is that the short, low-amplitude waves formed prior to sealing are three-dimensional in nature, distributed non-homogeneously in the span wise direction over the surface. Other subsidiary modes are subsequently formed, which merge to form new slugs like in the initial stage. Downstream in the pipe, the slug, surface displacements of various slopes and wave lengths are formed, subsequent to the strong interaction of the surface with the gas shear. It can also be noted that the initial wave mode formed before sealing are laterally inclined, and cannot be considered as sinusoidal waves. The last panel of the figure shows the instability of the wave crest as it seals, leading to strong surface wrinkling.

The blockage formed by the liquid causes more liquid accumulation with time, and this seems to further isolate the gas slugs. The mechanism repeats itself and successive slugs form along the pipe. Figure 4 shows the iso-contours of the free surface, combined with three velocity contours, each displayed on the 2D central y-z plane. These panels show something unusual,
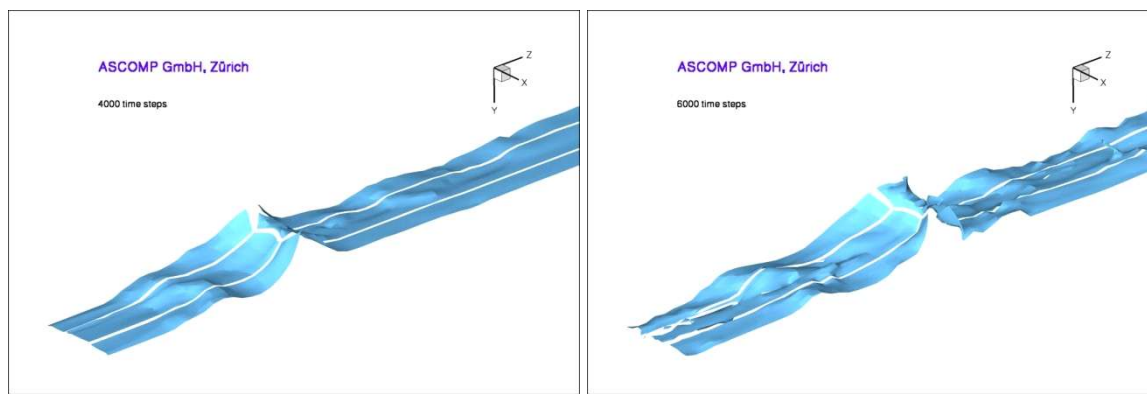
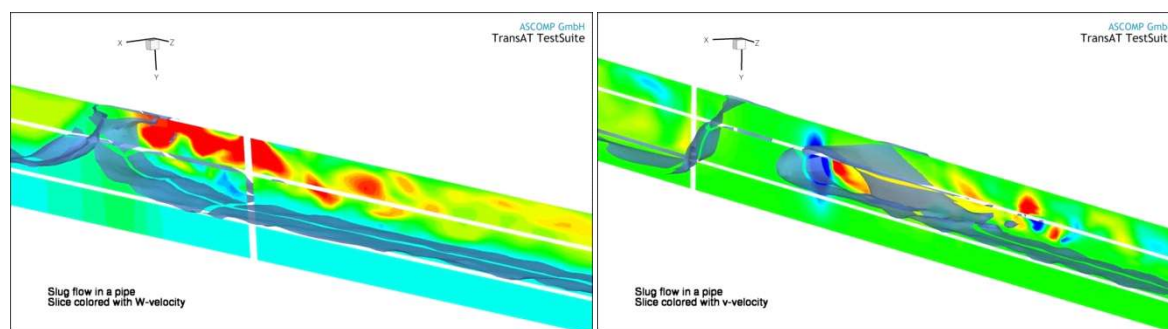**Figure 3.** Surface displacements at various time instants

Figure 4. Vortex shedding past the slug coloured by velocity fluctuations, highlighting wave breaking

that is the formation of vortex shedding past the slug, immediately after sealing. This observation is corroborated by all three instantaneous velocity- component contours, in particular w'. The mechanism is similar to what may be expected in flows past fixed blunt bodies; the slug plays somehow the same role, as it travels with a lower velocity than the gas after sealing. The breaking of the free surface after slug sealing is also perfectly illustrated in Fig. 4. Again, the panels combine free-surface and velocity iso-contours. The figure shows the vigorous plunging of the breaker after sealing, pretty much similar to what we observe in plunging breakers. The third panel shows the impact of the breaker over the stratified liquid surface, a region characterized by a very high level of turbulence production. Vortex shedding is again visible as in the previous panels, though the breaker seems to have affected the coherence of their motion.

The slug tail and centre speeds are discussed in Fig. 5 below, displaying the position of the slug versus time. A linear dependency is revealed, which is in agreement with the measurements of Martin *et al.* (2005), who obtained an average slug speed of U_s = 9.4 m/s, under these conditions. The slug speed is rather constant, as it has been found in the earlier 2D simulations (results not shown here). In case of the hydrodynamic slugging, the slug velocity can be calculated from gas and liquid flow rates if the void frac-

tion is known, in horizontal lines the mean velocity of the liquid in the body of the slug is approximately equal to the mixture velocity, or can be estimated analytically Collins *et al.* (1978) using:

$$U_S = 1.201 U_m + 0.532\sqrt{Dg\left(\rho_l - \rho_g\right)/\rho_l} \tag{3}$$
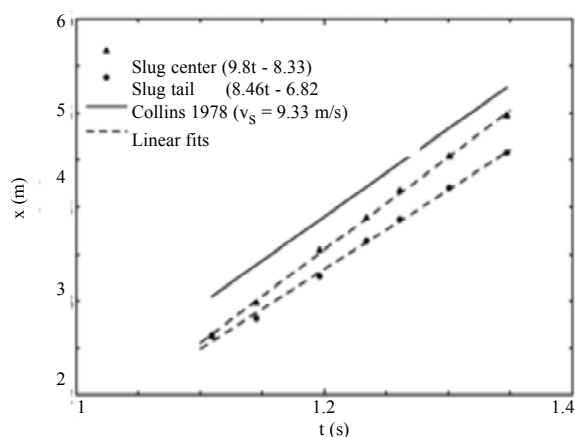

Figure 5. Slug speed (tail and centre): LEIS vs. analytical solution

where U_m stands for the mixture velocity. The result shown in Fig. 5 reveal that our LEIS simulation predicts the slug speed (tail and centre) in accord with the
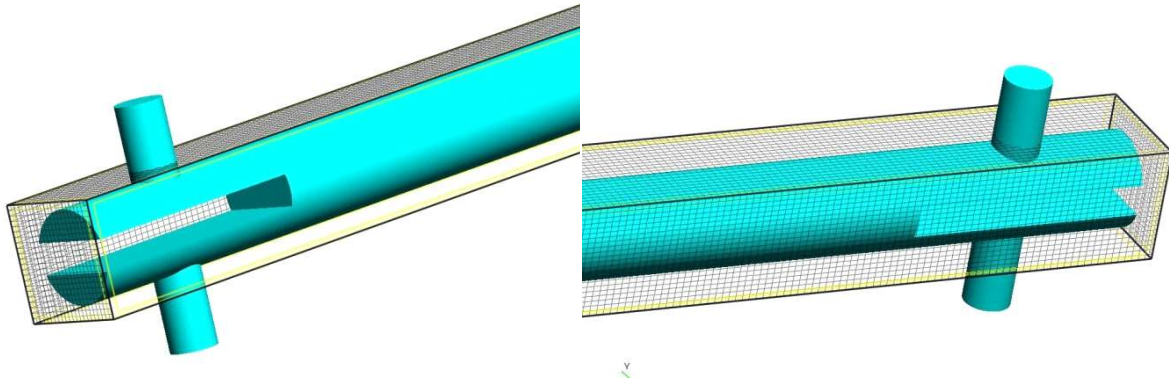
Figure 6. Computational IST grid. The CAD file is immersed in a cartesian grid

theory (3), which gives U_s=9.33 m/s, and experiment of (Martin *et al.* 2005) (U_s=9.4 m/s). This is an interesting result for practical applications, which shows that although a coarse grid has been used, the LEIS concept is capable to predict one of the most important flow features of pipe flows.

5. Slug Formation at the Wasp Facility

5.1 *Problem Description*

The experiments were performed at the Imperial College WASP facility with the test section mounted horizontally. Gas and water were fed from two different entries perpendicular to the main pipe (Fig. 6). Slugs were monitored from close to the point where they were first initiated until they decayed or exited the pipe. Twin-wire holdup probes were used to monitor the liquid level at a series of locations along the pipe. Slugs were discriminated from large waves by measuring the velocity using cross correlation of the outputs of successive probes (the waves travel at a lesser velocity that that of the mixture and slugs travel at a velocity higher than that of the mixture). The length of the stainless steel test section is 37 m and its diameter is 77.92 mm, the pressure at the outlet is 1 atm, and the temperature is 25oC. The liquid water is introduced below a stratification plate at the bottom of the test-line and the gas is introduced above it. The superficial velocities of the two phases (air and water) are: $U_{sL} = 0.611$ m/s and $U_{sG} = 4.64$ m/s, respectively.

5.2 *Simulation Setup*

Use was made here of the IST technique to mesh the pipe. The pipe CAD file was created using Rhinoceros software, and immersed into a Cartesian grid, as shown in Fig. 6. The 2D simulations were performed in a pipe of length 17 m. The 3D simulations were performed in a shorter domain of 8m, consisting of 715.0 cells, then in a longer one of 16 m, consisting of 1.200.000 cells. The simulation time for the 8 m pipe simulation was 10 days on a low bandwidth Dell

PC (2 nodes *x* 4 cores; Open MP parallel protocol) for 20s real time, and 53H on a high bandwidth 18 nodes IBM multicore computer (OpenMP protocol). The LEIS approach was employed here, with a filter width of 0.1D, combined with the Level-Set technique for interface tracking. Subscale modelling of turbulence was achieved with the k-ε model with filter width set equal to 0.1D (Labois, Lakehal 2011). The inflow boundary conditions involve fixing the superficial velocities and the void fraction, as specified in the experiment. Specifically at the inflow, we have set the following values for the turbulent flow conditions: gas superficial velocity $U_{sG} = 4.64$ m/s; liquid superficial velocity $U_{sL} = 0.611$ m/s; void fraction = 50%.

5.3 *Simulation Results (2D)*

Figure 7 shows the measured liquid hold-up at different probe locations along the axis: 5.01 m, 5.69 m, 6.99 m and 13.32 m. The signals display distinct large-wave structures developing along the pipe that could in fact be considered as slug-structures (Ujang 2003). While a traditional slug is a structure blocking the cross section of the pipe completely, large-wave structures with a length scale larger than the pipe diameter can also be termed as 'slugs'. The 3D simulations discussed next will help make the distinction between the different structures. Slugs or large-wave structures are captured around location $x = 3$ m and beyond (results not shown here). The periodicity of slug occurrence is clearly visible from these locations ($x > 5$ m). Figure 8 depicts the calculated water holdup in 2D at different probe locations along the axis, from 5.65 to 15 m. While the signal is qualitatively similar to the measured one in terms of slug or large-wave structures intermittency, it is unclear whether slugs were indeed captured; various locations exhibit water holdup of about $h_L/D = 0.8$-0.9. Be it as it may, large surface perturbations were already captured upstream close to the inflow, at $x = 0.76$m, while the experiment there shows liquid hold-up not exceeding $h_L/D = 0.2$. For the locations considered, the data and CFD provide a similar picture as to wave frequency.
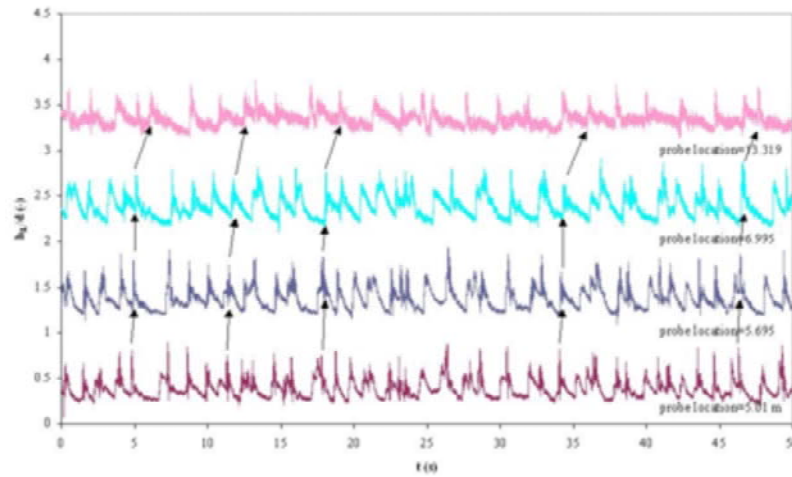
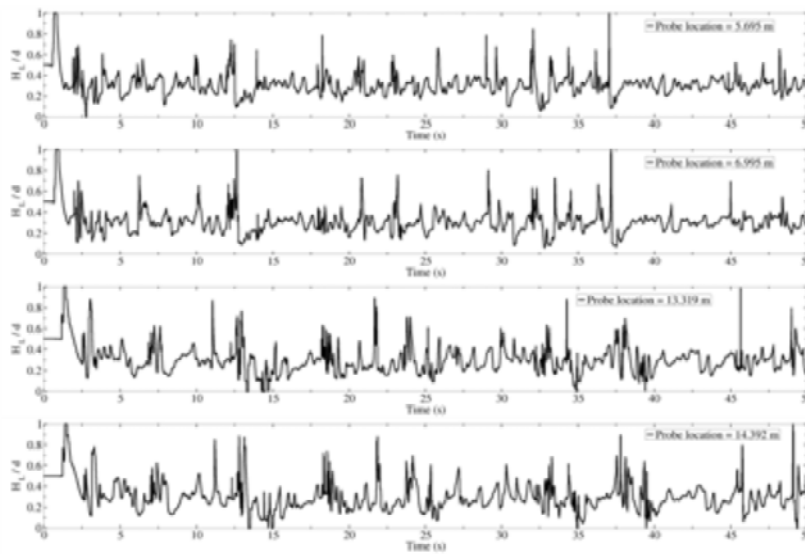**Figure 7.** Measured liquid holdup for $U_{sL} = 0.61$ m/s and $U_{sG} = 4.64$ m/s

Figure 8. Simulated liquid holdup for $U_{sL} = 0.611$ m/s and $U_{sG} = 4.64$ m/s

5.4 Simulation Results (3D)

To address the effect of pipe length the flow was reproduced in pipes with different lengths: 8 m and 16 m, using the same flow conditions. Figure 9 shows the development structures at different probe locations along the axis, at 5.01m, 5.695m and 6.995m. These were obtained from 3D simulations in the short pipe ($L = 8$ m). The distinct patterns at different locations show the variations in the slug frequencies. Slug frequency decays as the location of the probe is moved further downstream. Slugs or large-wave structures are predicted at downstream locations close to the pipe end: $x = 7$ m, in contrast to the experiment and longer-pipe simulations, both indicating a shorter position for the early slugs. Further, in contrast to the 2D results discussed earlier, slugs or large disturbances of the surfaces are not predicted upstream close to the inflow,

but downstream. These results are interpreted later on in terms of slug frequency, and compared to the longer pipe results.

Turning now to the 16m long pipe, the formation of the different types of slugs is well illustrated in Fig. 10. The first panel exhibits a 'large-scale slug', which, in the experiments is often referred to as 'operation slug'. This slug is formed upstream ($x < 3$ m) and fills entirely the pipe ($h_L/D = 1$) with an average size of the order of 2-4 D. Although the lower panels do not show a 100% water holdup filling the pipe as in the first one, the liquid structures are travelling at a higher speed than the mean flow, which makes them 'slugs'. Here one observes that gas bubbles are caught inside the slug, which explains that the measured liquid hold up h_L/D is less than unity (usually h_L/D is between 0.80 and 0.95).
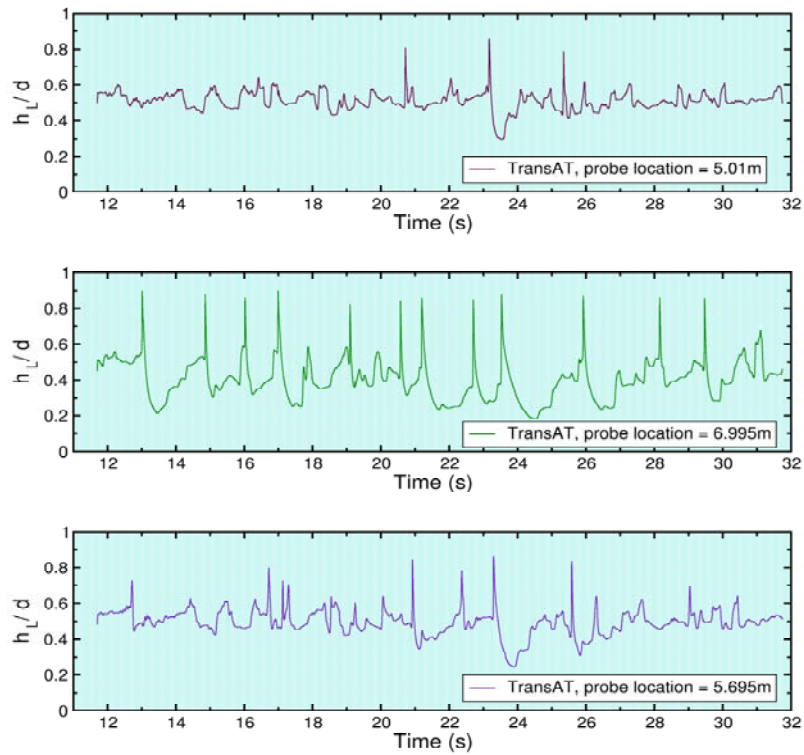
D. Lakehal, M. Labois, D. Caviezel and B. Belhouachi

Figure 9. Water holdup for the 3D simulation (short pipe: 8 m)
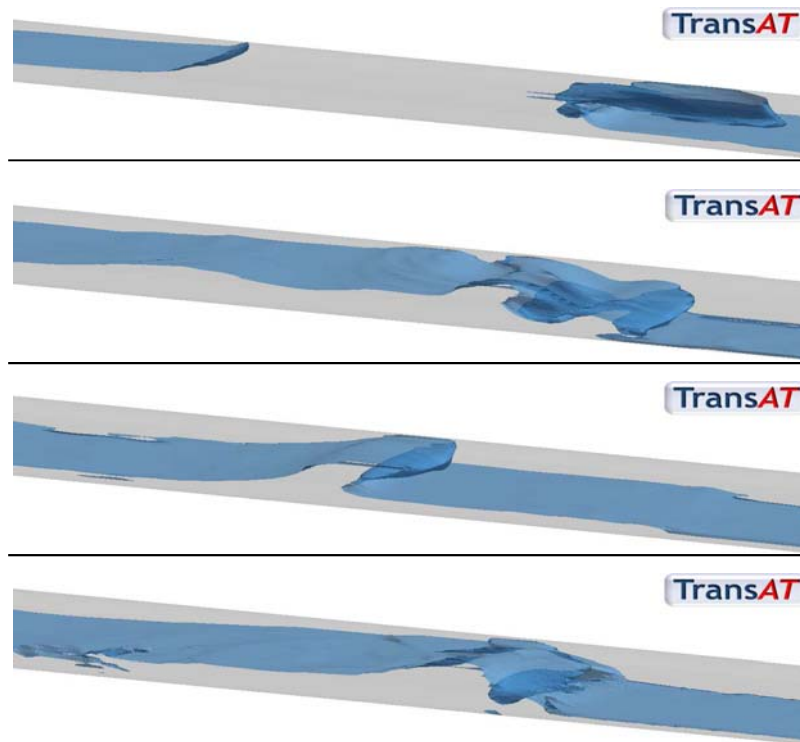

Figure 10. The formation of different kinds of slugs (long pipe: 16 m)

The slug- or large-wave structures frequency results shown in Fig. 11 are qualitatively similar to the structures observed in the experiment. The lines in green correspond to the 16m pipe simulations; the red ones to the 8m simulations; both in 3D. The shift in the fre-

quency peak observed for the two simulations is clearly due to the difference in pipe length, as the outflow boundary condition has an important impact on the flow. The frequency of the slugs is measured as a function of the abscissa. In the 16 m case, better
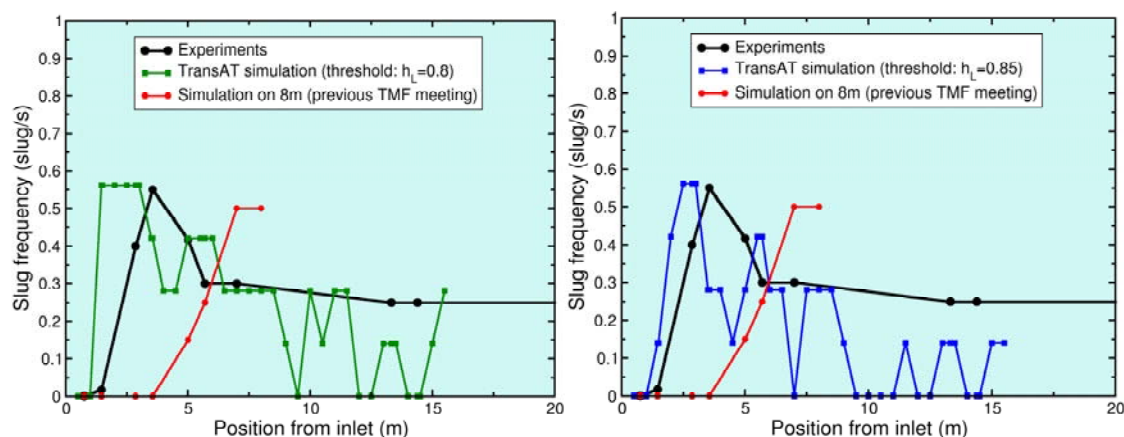
Transition of Gas-Liquid Stratified Flow in Oil Transport Pipes

Figure 11. Comparison of experiment and simulations of slug frequency for 2 pipe lengths; 8m and 16m. Left panel: threshold $h_L / D = 0.8$; Right panel: threshold $h_L / D = 0.85$

results are obtained as a peak frequency around 3.5 m can be seen, which is almost equal to the measured value. There is however a difference in terms of interpretation, when the frequency of slugs is evaluated based on h_L/D of 0.8 or 0.85. It is clear the simulation and measurement agree best for $h_L/D = 0.85$. Moreover, the evolution of the slug frequency along the axis of the pipe is in good agreement with the data, although the result suggests that the simulation time was not enough to acquire all the slugs with lower frequency (0.3 Slug/s). We thus conclude that the data.

Conclusions

The development of large-wave structures in gas-liquid 3D pipe flows has been examined using detailed CMFD simulations combining the Level-Set approach for interface tracking and VLES for turbulence modelling. The investigation complements earlier ones (Lakehal 2008) which had shown that the approach predicts more details of the flow as compared to the Eulerian two-fluid model, even if it is computationally expensive. Our predictions show that the ITM approach can be used for a one mile pipeline, using five million cells, which require a week of simulation on a 128 CPU cluster. The 3D turbulent flows simulations clearly provide a better picture of the flow, in particular regarding the onset of slug formation and frequency, the latter being predicted in accord with the experiment. From a practical standpoint, the results show that oil transport in a portion of pipelines can be approached more rigorously. The information from detailed 3D simulations could actually be employed to calibrate coarse-grained 1D lumped parameter models, which fail under other conditions than straight pipes. These detailed simulations should be ultimately coupled with a 1D code like OLGA; it could then be activated in fixed critical regions (*e.g.* over a hill).

References

Collins R, Moraes DE, Davidson JF, Harrison D (1978), The motion of a large gas bubble rising through liquid flowing in a tube. J. Fluid Mech. 89(3):497-514.

Hewitt GF (1982), Handbook of multiphase systems. Ed. G. Hestroni, Hemisphere /McGraw-Hill.

Labois M, Lakehal D (2011), Very-large eddy simulation (V-LES) of the flow across a tube bundle. Nucl. Eng. Design 241:2075-2085.

Lakehal D (2010), LEIS for the prediction of urbulent multifluid flows for thermal hydraulics applications. Nucl. Eng. Design 240:2096-2106.

Lakehal D (2008), Large-scale simulation of stratified gas-liquid flow transition and slug in oil pipes. 6th Int. Conf. CFD in Oil & Gas, Metallurgical & Process Industries, SINTEF/NTNU, Trondheim NORWAY.

Lakehal D, Meier M, Fulgosi M (2002), ITM for the prediction of interfacial dynamics and mass transfer in multiphase flows. Int. J. Heat & Fluid Flow 23:242-255.

Lin PY, Hanratty TJ (1986), Prediction of the initiation of slugs with linear stability theory. IJMF 12:79-98.

Liovic P, Lakehal D (2007), Interface-turbulence interactions in large-scale bubbling processes. Int. J. Heat & Fluid Flow 28:127-144.

Martin CS, Brown R, Brown J (2005), Condensation-induced hydraulic shock laboratory study. Final Report, (ASHRAE).

Sussman M, Smereka P, Osher S (1994), A level set approach for incompressible two-phase flow. JCP 114:146-158.

Taitel Y, Dukler AE (1976), A model for flow regime transitions in horizontal and near horizontal gas-liquid flow. AlChE J 22:47-55.

TransAT User Manual. ASCOMP GmbH, 2010. www.ascomp.ch/transat.

Ujang PM (2003), Studies of slug initiation and development in two-phase gas-liquid pipeline flow. PhD Thesis, University of London, London, UK.

Valluri P, Spelt PDM, Lawrence CJ, Hewitt GF (2008), Numerical simulation of the onset of slug initiation in laminar horizontal channel flow. IJMF 34:206-225.